

1

2 **LPJ-GM 1.0: Simulating migration**

3 **efficiently in a dynamic vegetation**

4 **model**

5

6

7

8 Lehsten, Veiko^{a,b}, Mischirow, Michael^b, Lindström, Erik^c, Lehsten, Dörte^b, Lischke, Heike^a

9

10 ^a Dynamic Macroecology/Land change science, Swiss Federal Institute for Forest, Snow and
11 Landscape Research WSL, Birmensdorf, Switzerland

12 ^b Department of Physical Geography and Ecosystem Science, Lund University, Lund, Sweden

13 ^c Centre for Mathematical Sciences, Department for Mathematics Lund University, Lund, Sweden

14

15

16 * Corresponding author: veiko.lehsten@gmail.com

17

18 **Abstract**

19 Dynamic global vegetation models are a common tool to assess the effect of climate and land use
20 change on vegetation. Though most applications of dynamic global vegetation models use plant
21 functional types, some also simulate species occurrences. While the current development aims to
22 include more processes, e.g. the nitrogen cycle, the models still typically assume an ample seed supply
23 allowing all species to establish once the climate conditions are suitable. Pollen studies have shown
24 that a number of plant species lag behind in occupying climatological suitable areas (e.g. after a
25 change in the climate) as they need to arrive at and establish in the newly suitable areas. Previous
26 attempts to implement migration in dynamic vegetation models have allowed simulating either only
27 small areas or have been implemented as post process, not allowing for feedbacks within the
28 vegetation. Here we present two novel methods simulating migrating and interacting tree species
29 which have the potential to be used for simulations of large areas. Both distribute seeds between grid
30 cells leading to individual establishment. The first method uses an approach based on Fast Fourier
31 Transforms while in the second approach we iteratively shift the seed production matrix and disperse
32 seeds with a given probability. While the former method is computationally faster, it does not allow
33 for modification of the seed dispersal kernel parameters with respect to terrain features, which the
34 latter method allows.

35 We evaluate the increase in computational demand of both methods. Since dispersal acts at a scale no
36 larger than 1 km, all dispersal simulations need to be performed at maximum at that scale. However,
37 with the current available computational power it is not feasible to simulate the local vegetation
38 dynamics of a large area at that scale. We present an option to decrease the required computational
39 costs, reducing the number of grid cells where the local dynamics is simulated only along migration
40 transects. Evaluation of species patterns and migration speeds shows that the simulation along
41 transects reduces the migration speed, and both methods applied, on the transects, produce reasonable
42 results. Furthermore, using the migration transects, both methods are sufficiently computationally
43 efficient to allow large scale DGVM simulations with migration.

44 **1. Introduction**

45 A large suite of dynamic global vegetation models (DGVMs) is currently used to simulate the effects
46 of climate and / or land use change on vegetation and ecosystem properties. These simulations result
47 in projections (or hind-casts) of species ranges as well as changes in ecosystem properties such as
48 carbon stocks and fluxes. Examples of these DGVMs include ORCHIDEE (Yue et al., 2018), LPJ-
49 GUESS (Sitch et al., 2003), IBIS (Foley et al., 1998), (Sato et al., 2007), for a review of DGVM
50 features see (Quillet et al., 2010).

51 While most DGVM applications use plant functional types (groups of plant species with similar traits
52 and responses to environmental conditions), here we only consider applications which explicitly
53 simulate tree species, e.g. (Hickler et al., 2012). These models typically assume that species can
54 establish at any site once the environmental conditions become suitable. However, in real ecosystems
55 species need not only to establish and replace existing vegetation, which the processes in gap models
56 describe successfully, but they also need to have a sufficient amount of seeds present at a given
57 location to successfully establish. Implicitly, current DGVMs assume that ample amounts of seeds of
58 all species are present in every location.

59 While this approach might seem reasonable in cases where the vegetation can keep up with climate
60 change (i.e. moving sufficiently fast to occupy areas which become suitable), there have been a
61 number of instances reported where a considerable migration lag occurred. For instance *Fagus*
62 *sylvatica* has been shown to have a considerable migration lag and is currently still in the process of
63 occupying its climatological optimum (Bradshaw and Lindbladh, 2005).

64 The implementation of migration into dynamic vegetation models is not only of interest for the
65 simulation of historical species ranges, it is also of interest for the projection of ecosystem properties
66 in the future since migration lags might lead to uncertainties in projected ecosystem properties if the
67 wrong species community is predicted to occur at a certain site (Neilson et al., 2005). Especially,
68 given that the speed at which environmental conditions change currently is unprecedented at least over
69 the last centuries, effects of the migration lag of key species should be evaluated when projecting
70 ecosystem properties. This holds in particular for projections over several centuries. For periods of
71 less than 50-100 years ahead, which corresponds to at most a few generations of most tree species, the
72 explicit modelling of seed dispersal might be less important for simulating tree distributions, in
73 particular when taking into account the overwhelming influence of human activities.

74 Migration lags can be caused by different factors. Seed transport might only occur over limited
75 distances. But also low seed amounts and in particular long generation times can slow down
76 migration. Seed amount and generation time depend on the competition with other trees: a free
77 standing tree starts earlier to produce seeds and produces more than a tree of the same age in a closed
78 forest. The competitors, however, are also migrating, which leads to feedbacks between the species
79 (Snell et al., 2014).

80 Thus, for simulations over large areas covering long time spans, species migration – consisting of a)
81 local dynamics influenced by the environment, b) competition between species, and c) seed dispersal –
82 has to be taken into account simultaneously for several species.

83 Species migration has been implemented successfully in dynamic vegetation models working on
84 smaller extents and finer scales than DGVMs typically use, e.g. forest landscape models (FLMs;

85 review in Shifley et al, 2017), such as TreeMig, (Lischke et al., 2006), Landclim (Schumacher *et al.*,
86 2004), Landis (Mladenoff, 2004), or Iland (Seidl et al., 2012) or spatially explicit individual based
87 models such as LAVESI (Kruse et al., 2018).

88 In these models, seed dispersal is modelled in a straightforward way: seeds are distributed from each
89 producing to each receiving cell with a distance dependent probability. However, transferring these
90 approaches to DGVMs is problematic, due to a number of conceptual and technical difficulties.
91 DGVMs usually operate on a coarse spatial resolution to reduce computational load and input data
92 requirements. This neglects the spatial heterogeneity within the grid cells. Additionally, and even more
93 critical for implementing migration, it leads to discretization errors: if it is assumed that the forest
94 representing the grid cell is located in the centre of the cell, the seeds cannot move far enough to leave
95 the cell (given a typical cell size of 50km by 50km or 10km by 10km). If, on the other hand, a
96 uniformly distributed forest in the cell is assumed in the simulation some seeds reach the neighbour
97 cell with each time step, leading to a resolution dependent speed up of migration.

98 Also some specifics of model implementations might complicate the inclusion of migration in some
99 DGVMs. Many DGVM implementations are done in a way that for each grid cell all years are
100 simulated before the simulation of the next cell is started. This is done to minimize input-output effort
101 since the whole climate data for each cell is read in at once and it also eases parallelisation for multi-
102 core computers, since in this case each node is assigned a number of grid cells which the node
103 calculates independently of the other nodes without communication. However, for simulating seed
104 dispersal, all cells need to be annually evaluated. Additionally to the reasons mentioned before, most
105 DGVM applications use plant functional types which comprise typically species with very different
106 traits with respect to migration (e.g. dispersal vectors or seed properties). Hence introducing migration
107 would require to split up PFTs into smaller groups and to parameterise the additional properties.

108 There have been a number of attempts to integrate species migration in DGVMs (cf. Snell *et al.*, 2014,
109 and Discussion section). For example, Sato and Ise (2012) developed a DGVM where species could
110 potentially migrate between neighbouring cells with a fixed rate of about 1km/year while Snell (2014)
111 simulated migration as an infection process between patches and within each grid cell.

112 However, to the knowledge of the authors, there is no implementation of a migration scheme into a
113 DGVM which allows simulations with a large extent, takes migration within the grid cell into account
114 and includes feedbacks between all simulated species.

115 Here we present two methods to fill this gap, i.e. allow simulating species migration of several species
116 simultaneously. The methods are implemented into the LPJ-GUESS DGVM but can potentially also
117 be implemented into other DGVMs. Though they are tested here using a virtual landscape, they can be
118 applied for simulations of large areas given current computing resources.

119 **2. Methods**

120 **2.1 The dynamic vegetation model LPJ-GUESS**

121 LPJ-GUESS is a flexible framework for modelling the dynamics of terrestrial ecosystems from
122 landscape to global scales (Sitch et al., 2003; Smith et al., 2001). Similar to most other DGVMs, it
123 requires time series of climate data (precipitation, air temperature and shortwave radiation), soil
124 conditions and carbon dioxide concentrations as input and explicitly simulates vegetation cover. While
125 it uses plant functional types in most applications, some applications simulate tree species (e.g.
126 Hickler et al., 2012; Lehsten et al., 2015). LPJ-GUESS explicitly simulates canopy conductance,
127 photosynthesis, phenology, and carbon allocation. It uses a detailed individual-based representation of
128 forest stand structure and dynamics. Each species (or PFT) has a specific growth form, leaf phenology,
129 life history and bioclimatic limits, determining its performance and competitive interactions under the
130 forcing conditions and realized ecosystem state of a particular grid cell (Sitch et al., 2003). A large
131 body of publications describes the features of LPJ-GUESS in detail; here we concentrate on the
132 changes that were applied to LPJ-GUESS version 4.0 (Lindeskog et al., 2013; Smith et al., 2014). To
133 differentiate between the original version of LPJ-GUESS and our extended version (where we
134 implemented the migration module) we refer to the extended version as LPJ-GM (short for LPJ-
135 GUESS-MIGRATION).

136 **2.2 Technical implementation**

137 Standard LPJ-GUESS simulations are typically performed at a computing cluster with cells running on
138 different nodes of the cluster without any interaction of the nodes. We implemented a distributed
139 simulation using MPI (Clarke et al., 1994) with the grid cells communicating with a master process.

140 Seeds are produced potentially in each grid cell at the end of each year after the first 100 years (see
141 below). The number of seeds produced is sent to the node computing the dispersal while all nodes wait
142 for this master node to finish the calculation. This node sends the number of seeds that arrive at each
143 grid cell back to all nodes to continue the calculation.

144 Similar to the standard version of LPJ-GUESS (Sitch et al., 2003; Smith et al., 2001), in the first 100
145 years no seed dispersal is performed and all species are allowed to establish and grow without seed
146 limitation and without N-limitation to equilibrate the soil pools with carbon and nitrogen. This time
147 period is used to sample NPP given a certain N deposition and climate to subsequently equilibrate the
148 N pools of the soil and a fast spin-up of 40000 years approximated using the sampled rates of C
149 assimilation (Smith et al., 2014). After this initialisation period all vegetation is killed and succession
150 starts from a bare soil and now seed limitation is active.

151 In LPJ-GM seed dispersal is done on an annual basis. The amount of seeds produced is communicated
152 to the master node at the end of each year. The master node re-distributes seeds over the whole spatial

153 domain according to the dispersal algorithm and communicates the amounts of arriving seeds back to
154 each grid cell. Seeds transferred to the grid cells are added to the seed bank which determines
155 establishment probability in environmentally-suitable cells (environmental suitability is determined by
156 means of environmental envelopes, containing amongst others minimum survival and establishment
157 temperatures; see Smith *et al.* 2001). All communications between the processes are done via MPI
158 protocol (Clarke *et al.*, 1994).

159 LPJ-GUESS is a gap model with the typical successional vegetation changes. To even out
160 successional based fluctuations in ecosystem properties and to be able to simulate disturbances most
161 previous applications simulate a certain number of replicate patches per grid cell. All patches share the
162 same climate but potentially differ in their successional stage due to different timing of disturbances
163 and stochastic mortality. Conceptually, each patch has a size of 1000 m² but represents an area
164 depending on the resolution of the grid cell. Patches have no spatial position with respect to each other
165 and do not interact (Smith *et al.*, 2001). In LPJ-GM we reduced the number of patches to one but
166 achieved the representative averaging by using explicitly placed small grid cells instead of statistical
167 units (replicate patches). For each large grid cell in the climate grid we simulate a large number of
168 cells of 1km² area resulting in a more than sufficient averaging of successional stages. LPJ-GUESS
169 simulations are typically performed with patch numbers around 10 (e.g. Smith *et al.*, 2001) but
170 depending on the aim of the simulation patch numbers have been increased even to 500 (e.g. Lehsten
171 *et al.*, 2016). In our setup even with 50 km corridors LPJ-GM represents a 0.5x0.5 degree cell with
172 200 simulation cells ranging at the higher end of the patch number per area compared to previous
173 simulations. We demonstrate this in Fig. 3 where a single 11 km by 11 km large grid cell is separated
174 in to 11 by 11 smaller grid cells with similar climate. The local dynamics and seed production is only
175 simulated along the transects (grey or green cells in left panel of Fig.3). As a next step the seed
176 production is interpolated onto all cells for which no local dynamics, was calculated and the seed
177 dispersal is simulated. Finally, seedling establishment is simulated, but only in the grid cells on the
178 corridors (more details for the different steps are given below).

179 **2.3 Migration processes**

180 **2.3.1 Seed production**

181 The seed production starts once the tree reaches maturity height and is scaled linearly with leaf area up
182 to maximum (LAI).

183 The seed number produced per tree is calculated as the product of the maximum fecundity multiplied
184 by the proportion of the current LAI to the maximum LAI and multiplied by the area per grid cell. For
185 example, the maximum fecundity of beech is 29000, the maximum LAI is 5 m² *m⁻² and the maturity
186 height is 14.4 m. Hence a tree of 15m height is above the maturity height, and with an LAI of 2.5 m²
187 *m⁻² it will produce 29000*0.5/5=14500 seeds. No specific age of maturity is taken into account.

188 All seeds of a species produced $S(x',y')$ at a location (x',y') within a year are available for seed
 189 dispersal. Once seeds have entered the seed bank, no further dispersal is possible (they remain in the
 190 seed bank). Though LPJ-GUESS keeps track of carbon allocated to the main plant compartments and
 191 even allocates a certain amount of carbon to seeds (which is transferred to the litter pool, the soil pool
 192 and finally the atmosphere), for simplicity we decided not to relate the seed production to the carbon
 193 accounting at this point. Allocation rules including seed production and even mast fruiting effects
 194 (synchronised strong increases in seed production e.g. similar to Lischke *et al.* 2006) could be
 195 included in the future.

196 **2.3.2 Seed dispersal**
 197 The produced seeds are distributed according to

198
$$S_d(x,y) = \int S(x',y') k_s(x - x', y - y') dx' dy' \quad (\text{eq. 1}).$$

199 $S(x',y')$ is the seed production, and $k_s(x - x', y - y')$ the seed dispersal kernel in euclidean
 200 coordinates. The seed distribution $S_d(x,y)$, i.e. the input of seeds in location x, y is then obtained by
 201 integrating over all possible locations x', y' for arriving at x, y .

202 Thus, the seed distribution is given by the convolution $(\ast\ast)$ of the seed production and the seed
 203 dispersal kernel:

204
$$S_d = S \ast\ast k_s. \quad (\text{eq. 2})$$

205
 206 For this study we used the seed dispersal kernel and parameterization for *Fagus sylvatica* from
 207 TreeMig (Lischke *et al.*, 2006). The seed dispersal kernel defines the probability of seeds arriving at a
 208 sink cell (x,y) from the source cell (x',y') with a certain distance $z = \sqrt{(x - x')^2 + (y - y')^2}$.

209 The kernel is specified in a polar coordinate system,

210 $k_s(z, \theta) = k_s(z|\theta)k_s(\theta)$, with the radial distance z . The seeds follow a mixture of two exponential
 211 distributions, the short and the long term dispersal, while the angular dispersion, θ , is uniform in all
 212 directions (in our case the angular dispersion θ is uniform, but if one is interested e.g. in implementing
 213 wind directions this can be changed). Thus, the radial component of the kernel is given by

214
$$k_s(z|\theta) = (1 - \kappa) \frac{1}{\alpha_{s,1}} e^{-\frac{z}{\alpha_{s,1}}} + \kappa \frac{1}{\alpha_{s,2}} e^{-\frac{z}{\alpha_{s,2}}}, \kappa \in (0,1) \quad (\text{eq. 3})$$

215 while the angular term is given by

216
$$k_s(\theta) = \frac{1}{2\pi} \text{ for } \theta \in [0, 2\pi] \quad (\text{eq. 4.1})$$

218 $k_s(\theta) = 0 \text{ otherwise} .$ (eq. 4.2)

219

220 The dispersal kernel is defined by the species specific values for the proportion of long distance
221 dispersal κ and the species expected dispersal distances $\alpha_{s,1}$ and $\alpha_{s,2}$ for the two kernels.

222 The species specific values for these parameters (0.99 for κ_s and 25m and 200m for the two mean
223 dispersal distances k_s for *Fagus sylvatica*) were taken from by Lischke *et al.* (2006).

224 **2.3.3 Seed bank dynamics**

225 The number of the seeds in the seed bank (i.e. the dormant seeds in the soil that can germinate in
226 subsequent years in each cell) is increased by the influx S_d of seeds according to (eq. 1), and reduced
227 by the yearly loss of germinability (caused by decay of seeds; see supplementary material 4 for
228 parameter values) and the amount of germinated seeds at the end of each simulated year, similar to
229 TreeMig (Lischke et al., 2006).

230 For each grid cell and each year we prescribe whether the species requires seeds to establish. By not
231 requiring seeds for establishment we define refugia, or we define that the species' seeds are known to
232 be very far dispersed and hence no explicit simulation of establishment by seeds is required for this
233 species. Technically this is implemented by reading in a list for each cell containing a year from which
234 onwards a species' establishment is not limited by the availability of seeds.

235 **2.3.4 Germination**

236 LPJ-GUESS is a gap model and in the original version the number of newly established saplings only
237 depends on the amount of light reaching the forest floor (given that the cell has a suitable climate). In
238 LPG-GM we additionally limit the establishment of seedlings depending stochastically on the number
239 of available seeds. Hence the seed limitation is applied before the light limitation. The probability that
240 a species establishes is given in equation 5.

241 $P_{est} = S p_x P_{germ}$ (eq. 5)

242 Where the P_{est} is the probability of the species establishing, S is the number of seeds and P_{germ} is the
243 seed germination proportion. The extra parameter p_x takes (implicitly) the area of each grid cell into
244 account. In our case we fixed this parameter to 0.01 after initial testing. Hence if in a certain year 100
245 seeds are in the seed bank and the germination rate is 0.71 (value for *Fagus sylvatica*) the probability
246 of establishment is $0.01*100*0.71=0.71$.

247 **2.4 Enhanced dispersal simulation**

248 One way to simulate seed dispersal is to calculate the convolution of the matrix containing the seed
249 production and the seed dispersal kernel (specified in eq. 1 and eq. 3). However, evaluating the
250 convolution explicitly can be computationally expensive for seed dispersal kernels with long range.

251 **2.4.1 Fast Fourier transformation method (FFTM)**

252 An alternative is based on the convolution theorem and the Fast Fourier Transformation (FFT), a
253 technique commonly used in physics, image processing and engineering (Strang, 1994), but rarely in
254 ecology or (see e.g. Powell, (2001) Shaw et al., (2006), Pueyo et al., (2008)).

255 This approach carries out the computations in the frequency domain, see Gonzales & Woods (2002).

256 Here we use the notation $F\{S\} = \int e^{-iux-ivy} S(x, y) dx dy$ to denote the two dimensional Fourier
257 transform of S and correspondingly $F\{k_s\}$ the two dimensional Fourier transform of k_s . It then follows
258 that the Fourier transform of the convolution equals the product of the Fourier transforms

259
$$F\{S ** k_s\} = F\{S\}F\{k_s\} \quad (\text{eq. 6})$$

260 Thus, it is possible to compute the convolution by applying the inverse Fourier transform to the
261 products of the Fourier transforms

262
$$S ** k_s = F^{-1}\{F\{S\}F\{k_s\}\} \quad (\text{eq. 7})$$

263 This equation must be discretized before evaluating it on a computer. The discrete Fourier transform is
264 computed using the Fast Fourier Transform (Cooley and Tukey, 1965), which has a computational
265 cost of $O(N^2 \log^2(N))$ in two dimensions. The discrete approximation of S_d is then given by

266
$$S_d = F^{-1}\{F\{S\} \odot F\{k_s\}\} \quad (\text{eq. 8})$$

267 where \odot is the element-wise (Hadamard product) multiplication of matrices.

268 Nowadays, software packages for FFT typically only compute positive frequencies. That means that
269 we have to shift the frequencies prior to the element-wise multiplication of $F\{S\}$ and $F\{k_s\}$. This is
270 illustrated in Fig.1, see also supplementary material S.2.

271

272 <Figure 1 to be placed here>

273 While this method allows including different wind distributions by changing the seed dispersal kernel
274 (as long as they are valid for the whole simulated area), it does not allow to use different seed dispersal
275 kernels at different locations, e.g. due to prevailing wind directions in valleys, due to barriers to animal
276 transport like a motorway, or due to lower transport permeability in already forested areas.

277 **2.4.2 Seed matrix shifting method (SMSM)**
278 Another way to simulate seed dispersal is to simulate the seed movement between the cells explicitly
279 by shifting the matrix containing the produced seeds by one position (repeatedly in all directions of the
280 Moore neighbourhood; i.e. the surrounding eight cells) and simulating seed transport of a certain
281 proportion of the seeds into the next cell. Each move can be viewed as an independent random
282 variable. Repeating these moves thus corresponds to a random walk process. The Lindeberg's
283 condition for sequences for sums of independent random variables ensures that the kernel will be
284 Gaussian under general conditions (Shiryayev, 2016), with the expected value given by the sum of
285 expected values for each random variable and similarly for the variance (see supplementary material
286 S.1 for a formal proof and a derivation of the parameters of the resulting normal distribution).

287 If this is done repeatedly it allows an easy implementation of spatial explicit differences in seed
288 dispersal kernel distributions, by adjusting the proportions of seeds being transported into the next cell
289 according to a similarly sized matrix containing the area roughness or permeability. By this approach,
290 barriers and even wind speeds in latitudinal and longitudinal directions can be implemented by
291 adjusting the dispersal probabilities accordingly. After the distribution of the dispersed seeds is
292 calculated, the seeds are added to the seed bank. An example calculation of the first three steps of the
293 SMSM (in the final simulation 10 steps are performed) is given in the Supplement S.3.

294 **2.5 Corridors**
295 Seed dispersal acts at a rather fine scale compared to the usual scale at which DGVMs are run (LPJ-
296 GUESS is typically run at a 0.5 to 0.1 degree longitude / latitude scale), though some regional
297 applications use finer grids (e.g. Scherstjanoi et al., 2014). Given that the average long distance seed
298 dispersal for example for *Fagus sylvatica* is 200 m (representing 0.002 degree longitude / latitude at
299 the Equator), simulations at such a coarse scale will not be able to capture this process.

300 As a compromise between currently available computing resources and required simulation detail we
301 choose a 1km scale at which we performed our simulations. However, even at this scale, simulating
302 large areas for example within the European continent would result in a high computational effort.

303 Given that in some areas the landscape is rather homogenous while other areas have a variable terrain
304 (or land use conditions), we test whether for homogenous landscapes it is sufficient to simulate the
305 local dynamics only in latitudinal, longitudinal and diagonal transects (i.e. north-south, east west, as
306 well as, northeast-southwest and northwest-southeast corridors) and how this will influence the
307 migration speed. The corridors are 1 grid cell wide and regularly placed in the simulation domain.
308 Their density can be chosen by defining the distance between the latitudinal and longitudinal
309 corridors.

310 Although LPJ-GM only simulates local dynamics in the cells along the corridors, the seed matrix
311 needed to be filled for the dispersal calculation using the FFTM or the SMSM algorithm. We applied a
312 nearest neighbour interpolation of the seed production before performing the seed dispersal calculation
313 (theoretical considerations show that a distance weighted average would strongly speed up the
314 migration).

315 **2.6 Simulation experiments**

316 To test our newly developed migration module we simulated the spread of a single late successional
317 species (*Fagus sylvatica*) through an area covered by an early successional species (*Betula pendula*).
318 The species specific parameters for both species are given in the Supplement S.4. All grid cells and all
319 years in the simulated area had a static climate suitable for both species. Though the simulated domain
320 is quadratic in our case it could have any shape. Each cell in the simulated domain has been simulated
321 independently (except for the influx and outflux of seeds) from each other. For one specific simulation
322 using the SMSM method we assumed differences in the dispersal ability (e.g. more or less permeable
323 areas or physical barriers) while the climate on all grid cells is still static and favourable. The dispersal
324 ability of the landscape is displayed in Fig. 2. Areas colored white have zero permeability, hence no
325 seeds can reach these areas.

326

327 <Fig. 2 placed here>

328

329 Figure 3 demonstrates the sequence of simulating vegetation dynamics on the corridors, interpolation
330 of seed production, seed dispersal on the entire grid and back via the seed input on the transects.

331 <Fig. 3 placed here>

332

333 Given the uniformity of the climate, there should be no variability in the migration speed caused by
334 differences in climatic conditions. We simulated the spread of *F. sylvatica* from a single grid cell in
335 the corner of the study area which represents the refugium. We tested several corridor distances
336 (between the parallel and between the diagonal corridors) for their effect on the migration speed. To
337 calculate the migration speed we first determined the migration distance. This was the distance
338 between the start point of the migration and the 95-percentile farthest point in the virtual landscape
339 where the leaf area index (LAI) of *F. sylvatica* was larger than 0.5. This migration distance was
340 subsequently divided by the simulated time elapsed since the start of the migration. To avoid founder
341 effects we neglected all points within first 5 km from the starting location (the refugium). The
342 simulations were performed over 3000 years and over an area of 100 by 100 cells of 1 km². Finally we

343 ran one simulation where we did not calculate the seed dispersal (but performed all communication
344 between cells and one run even without the communication), hence allowing us to estimate the
345 computation time demand for the seed dispersal calculation.

346 **2.7 Performance evaluations**

347 To estimate the performance of our methods against an implementation in which each grid cell
348 exchanges seeds with each other we developed a Matlab® script, since initial testing had shown that
349 such a procedure would be too slow to be implemented in LPJ-GUESS. Hence when evaluating the
350 performance differences from the script one has to bear in mind that these are calculated in a different
351 environment. However in a general sense we can see no reason why they should not reflect the
352 performance differences between the algorithms. The whole Matlab® script testing the performance
353 including the graphs is part of the Supplementary material.

354 **3. Results**

355 **3.1 Explicit seed dispersal**

356 The study comparing the performance of different migration mechanisms without the vegetation
357 dynamics, implemented in Matlab®, has shown that both the FFTM as well as the SMSM were
358 performing faster than the explicit dispersal from each grid cell to each other within the range of the
359 dispersal (last figure Supplement 2). This was especially pronounced if the area to be simulated was
360 increased. Though faster than the explicit dispersal method, the SMSM was still up to an order of
361 magnitude slower than the FFTM, in particular for large simulations domains in Matlab® while the
362 FFTM and the SMSM required relatively similar amounts of time in the implementation in LPJ-
363 GUESS (tab.1).

364 **3.2 FFTM simulations**

365 Using the parameterization from TreeMig in a complete (no corridors) simulation area of 100 by 100
366 grid cells with the size of 1km² each resulted in a migration speed of 34 m per year for *Fagus sylvatica*
367 (Fig. 4).

368 <Figure 4 placed here>

369 Though the establishment in the model is stochastic, the simulated spread was relatively smooth. The
370 corridor distance of 10 km, 20 km and 50 km resulted in a reduced migration rate of 26, 28 and 28
371 m/year (compared to a simulation without corridors), respectively (Fig. 4, lower three rows of panels).
372 While in the simulation without corridors the variability of the migration speed was relatively low
373 (dots under the red line in upper left panel of Fig. 4), this variability was strongly increased when
374 corridors were simulated. This was caused by *F. sylvatica* migrating along the diagonal, reaching the

375 end point of the diagonal and then migrating along the longitudinal and latitudinal corridors into cells
376 which had actually a shorter distance to the refugia than the endpoint of the diagonal.

377 The simulation time per grid cell in the whole area (range for which the seed dispersal was computed)
378 was increased by 12% by simulating the FFFT, but by using the corridors it was reduced to 36%,
379 22% and 12%, compared to simulating the full area (Tab. 1, col. 7). The proportion of computation
380 time used to perform the FFFT increased from 11% without corridors to 18%, 29% and 29% for
381 simulations with corridors every 10, 20 and 50 km. This estimate only includes the required time for
382 computing the FFT-based seed dispersal since the control run without seed dispersal still contained all
383 communication between cells. For the control run seeds were produced and sent to the master but the
384 master did not compute the seed dispersal, though still communicated with all other nodes to allow a
385 fair assessment of the computation time demand of the two methods (see Tab. 1). An additional run
386 without any communication resulted in a computation time similar to the run with communication.

387 **3.3 Shifting seed simulations**

388 Initial testing of the probability parameter for the SMSM suggested a value of $p=5 * 10^{-7}$ to generate a
389 migration speed comparable to the migration speed for the FFFT based on the TreeMig
390 parameterization. Using the derivation presented in supplement 2 it is possible to calculate this
391 parameter for a Gaussian dispersal kernel. One can approximate any dispersal kernel by adding several
392 Gaussian kernel, however this would increase calculation time since the SMSM would have to be
393 performed several times. Therefore we decided to choose a parameter for the SMSM approximating
394 the migration speed rather than the seed dispersal kernel used in Lischke *et al.* (2006). This resulted in
395 a migration speed of 39 m/year for the filled area and 27m/year respective 29 m/year and 30m/year for
396 the 10 km, 20 km and 50km corridors (Fig. 5).

397 <Figure 5 placed here>

398 Similarly to the FFFT simulations, the migration speed was reduced for simulations with transects
399 (see table 1 for a summary). Also comparable to the FFFT based seed dispersal computation,
400 calculation time per grid cell in the whole area (range for which the seed dispersal is computed) was
401 increased by 16% by the simulation of dispersal, but reduced to 35%, 19% and 11% by using the
402 corridors. The proportion of calculation time spent for simulating the seed dispersal is comparable to
403 the proportion using the FFT, it was 16%, 19%, close to 23% and 32% (see Tab. 1).

404 Since the SMSM allows adjusting the probability depending on the seed transport permeability of the
405 terrain we also simulated the migration within a non-homogenous dispersal area. The results of this
406 simulation are displayed in Fig 6. The total computation time for this simulation was 46000 CPU*h
407 for 6000 years.

408

409 <Figure 6 placed here>

410 Though all cells of the virtual landscape had a similar climate, some cells were never occupied (see
411 Fig. 6) because the seeds were not able to reach them due to the different permeability (which might
412 not be reasonable for real world simulations but demonstrates the method). Migration speed was
413 different in different parts of the simulated area.

414 <Table 1 placed here>

415

416 **4. Discussion**

417 To our knowledge, in our study for the first time (tree) species migration has been implemented in a
418 DGVM in a way that allows simulations of simultaneously migrating and interacting species for large
419 areas.

420 **4.1 Performance of new migration methods**

421 The presented new methods for simulating migration in DGVMs showed a promising performance in
422 different aspects.

423 The first is the gain of efficiency by the FFFT and the SMSM methods as compared to the traditional,
424 straightforward approach to evaluate the seed transport from each cell to each other (last Fig in S.2). A
425 two dimensional FFT can be obtained by successive passes of the one dimensional FFT, hence the
426 complexity will be the one-dimensional complexity squared (Gonzalez and Woods, 2002).The
427 computational complexity for the FFFT is $O(N^2 \log^2(N))$ for a $N \times N$ grid discretizing the seed
428 distribution, while the complexity of the direct implementation of the convolution approach in the
429 SMSM is $O(2KRN^2)$ for a $N \times N$ grid discretizing the seed distribution and $R \times R$ kernel with K
430 being the number of iterations of the SMSM (for the derivation see supplementary material S.1). This
431 can be computationally comparable to the FFFT for kernels with short range of R . Secondly,
432 simulating the local dynamics only along the corridors instead of in the full area resulted in a similar
433 migration pattern, and the simulated migration speed was similar to that of the simulation with full
434 grid cell cover (though it is slower, caused by the stochasticity of the establishment, see table 1), but
435 needed much less computing time (reduction of 88% for the corridors every 50km).

436 **4.2 Comparison of the two dispersal methods**

437 In this study we present two alternative methods for simulating dispersal, which differ in their
438 properties. While the FFFT allows any type of seed dispersal kernel, the SMSM corresponds to a
439 normal distribution kernel. Although other shapes of dispersal kernels can be approximated by
440 weighted sums of normal distributions, of which each of them has to be simulated by an own SMSM,
441 which will cause strong increases in computational demand. Additionally the SMSM restricts the long
442 tail of the distributions by the number of iterations, as the seeds can travel only one grid cell per
443 iteration step.

444 On the other hand, the advantage of the SMSM lies in its ability (contrary to the FFFT) to modify the
445 parameters of the seed dispersal kernel spatially, depending on the terrain. If instead of applying a
446 single permeability for all directions, a different permeability is applied for each of the 8 directions
447 (e.g. north, northeast, east, etc.) this method also allows a spatially explicit consideration of wind
448 directions (which is not possible for the FFFT, as it relies on a universal kernel applied to the entire
449 area). Hence, depending on the aim of the analysis either one or the other or a combination of the
450 algorithms is most suitable.

451 While not implemented here, it should be theoretically possible to use the FFTM (preferably with
452 corridors) for some homogenous parts of the simulated area and the SMSM for the remaining part in a
453 single simulation. As long as the seed donor areas for both methods are exclusive, and the areas in
454 which the seeds are allowed to disperse overlap at least with the width of the kernel, we can see no
455 reasons why this should not be feasible.

456 **4.3 Comparison to other approaches**

457 Our new species migration submodule FFTM uses for the first time an algorithm based on Fast Fourier
458 Transformation to simulate dispersal in a DGVM. Due to its efficiency, the FFT one of the
459 “workhorses” in mathematics, physics and signal processing (Strang, 1994). In ecology, there have
460 been a few applications using FFTs to simulate dispersal of pollen (e.g. for risk analysis, Shaw et al.
461 (2006), seeds (Pueyo et al., 2008) or even in a course compendium (Powell, 2001b)), but not as a
462 standard technique in DGVMs.

463 The SMSM, in turn, mimics the seed transport process itself in a simple and straightforward way,
464 which to our knowledge has also not been implemented in DGVMs either.

465 Both approaches are combined with features of modelling species migration that are already used in
466 other dynamic vegetation models (cf . Snell, 2014).

467 The cellular automaton KISSMig (Nobis & Normand, 2014), e.g. simulates the spread of single
468 species driven by a spatio-temporal grid of suitability, and by transitions to the nearest neighbour cells,
469 which is similar to one iteration in the SMSM. The suitability based models CATS (Dullinger *et al.*,
470 2012) or MigClim (Engler and Guisan, 2009) simulate a simple demography of single species and
471 explicitly the spread based on a seed dispersal kernel.

472 To also account for ecophysiology, the CATS model was combined with LPJ-GUESS in a post-
473 processing approach (Lehsten *et al.*, 2014). A spatio-temporally explicit suitability for a single species
474 was estimated from LPJ-GUESS simulations of the productivity of this species, assuming the presence
475 of the other species. This suitability was subsequently used within CATS to simulate migration. Such
476 a post-processing approach however does not include interactions between several migrating species.

477 Forest landscape models have been developed to integrate such feedbacks between species as well as
478 dispersal (He et al., 2017; Shifley et al., 2017). These models simulate local vegetation dynamics with
479 species interactions, and dispersal by explicit calculation of seed or seedling transport probabilities
480 with dispersal kernels of different shapes (e.g. LandClim (Schumacher *et al.*, 2004), Landis
481 (Mladenoff, 2004), Iland (Seidl et al., 2012)). To capture spatial heterogeneity, they run at a
482 comparably fine spatial resolution (about 20-100m grid cells), allowing only the simulation of
483 relatively small areas due to computational demands.

484 To overcome such computational limits, several approaches for a spatial upscaling of the models have
485 been put forward. For example, the forest landscape model TreeMig can operate at a coarser resolution
486 (grid cell size 1000m) because it aggregates the within-stand- heterogeneity by dynamic distributions
487 and height classes (Lischke *et al.*, 1998), which allows applications at a larger scale, e.g. over entire
488 Switzerland (Bugmann *et al.*, 2014) or on a transect through Siberia (Epstein *et al.*, 2007). Another
489 upscaling of TreeMig was achieved by the D2C method (Nabel, 2015; Nabel and Lischke, 2013)
490 which simulates local vegetation dynamics only in a subset of cells that are dynamically determined as
491 representative for classes of similar cells. This method led to a computing time reduction of 30-85%
492 compared to the full simulation. This reduction is in a similar range for our transect method depending
493 on the configuration of the corridors.

494 In DGVMs, the discretization problem resulting from the need to upscale from the fine scale at which
495 migration processes act to the scale at which DGVMs work is very pronounced, because they are
496 designed to operate on very large extents (continents or the entire globe). Given the computational
497 demands of the simulations, they are therefore typically running at a coarse resolution for example 0.5
498 or 0.1 degree longitude / latitude, and simulate the vegetation dynamics at the centre of each of these
499 grid cells, assuming this point to be representative for the entire cell.

500 Snell (2014) approached the discretization problem for the DGVM LPJ-GUESS by assuming that the
501 numerous replicates of the vegetation dynamics on a patch are randomly distributed over the area of
502 the grid cell (using 400 patches). Migration within the grid cell is treated similar to an infection
503 process, where the probability of a patch becoming infected (e.g. of the migrating species being able to
504 establish) depends only on the number of already invaded patches within the grid cell. Only once a
505 migrating species managed to establish in a certain proportion of the patches of the simulated grid cell,
506 further dispersal (explicit via a dispersal kernel) into surrounding grid cells is possible. Yet, there is no
507 spatial orientation of the patches within the grid cell and all simulations in this approach are strongly
508 resolution dependent. Simulations of large areas such as continents remain computational challenging
509 with this approach.

510 Our transect approach, similarly to the approach of Snell (2014), uses smaller representative spatial
511 units, 1km-cells, for a spatial upscaling. Since these small grid cells are arranged in contiguous
512 corridors, the migration along these corridors can be simulated without or with only a small
513 discretization error. The results indicate that also the error potentially introduced by the interpolation
514 to the rest of the area is small.

515 The two approaches that we present differ in their ability to simulate heterogeneous landscapes (in
516 terms of permeability). We suggest using the FFTM with corridors in homogenous landscapes (to
517 speed up the computation) and to use the SMSM without corridors in heterogeneous landscapes. In
518 cases where parts of the domain are heterogeneous (e.g. the regions around a mountainous area) and

519 other, homogenous parts (e.g. lowlands), the cells can be arranged in a way that they cover the whole
520 area in the heterogeneous part and only corridors in the homogenous part. In this setting the SMSM
521 can still be used for the whole domain and an improvement of computation time can be achieved by
522 only simulating the local vegetation dynamics in the homogenous parts of the domain. Thus, with our
523 approaches, we have combined several advantages of the before mentioned approaches: the seed
524 dispersal from forest landscape models, improved by the novel FFTM or SMSM and the
525 ecophysiology, structure and community dynamics of LPJ-GUESS. We furthermore found a
526 compromise between discretization and efficiency by the corridor method.

527 **4.4 Potential further improvements**

528 Despite the satisfying performance of the new methods in these first tests some aspects suggest further
529 development.

530 **4.4.1 Computation time**

531 Even with the computing time reduction by the corridor approach using a corridor of 50km distance,
532 the computing time required for the simulations including dispersal was still considerable. The reason
533 is that the number of cells on the corridors (where the local dynamics are simulated) is larger than the
534 number of replicates usually used in all the 1 or 0.5 degree grid cells simulated in traditional DGVMs.
535 For large-scale applications, the approach should be further optimized, e.g. by choosing corridors
536 even further apart from each other in homogenous areas and adapting the corridor density to the large
537 scale (between grid-cell) heterogeneity of the terrain. The within grid-cell heterogeneity in turn can be
538 accounted for by deriving seed dispersal permeability, that can be used in the SMSM approach.
539 Another area of improvement lies in the technical implementation of the seed dispersal algorithm. In
540 the current implementation, the seed dispersal is performed at a single cpu, while all other cpus wait
541 until they receive the seeds. There are certainly ways to perform the seed dispersal computation on
542 several nodes to decrease the waiting time. Furthermore, in multi-species simulations the dispersal has
543 to be calculated for each migrating species. In this case, the dispersal of different species should be
544 calculated on separate nodes. Enlarging simulation areas generally resulted in longer runtimes for all
545 methods. Sometimes, however, the runtimes decreased in a pronounced way for the FFTM
546 (supplementary material, S.2). A cause for these decreases is that the efficiency of the FFT depends on
547 possible factorizations of the domain size (Bronstein, I.N., Semendjajew, K.A., Musiol, C., Mühlig,
548 1995). For example, it is most efficient for domain sizes of 2^n . Thus, a careful choice of the domain
549 size or of an FFT code doing that automatically promises to speed up the FFTM. The last figure in S.2
550 does not represent the differences in computation time between SMSM and FFTM as they are
551 measured on the computing cluster when performing the actual simulation. While in table 1, there was
552 only a marginal difference between the calculations of the two methods, the differences in the
553 Matlab® implementation presented in S.2 are up to an order of magnitude. It seems that Matlab® uses

554 a different optimization for calculating the Fast Fourier transformation even though both Matlab® as
555 well as the FFT libraries used on the computing cluster are based on the libraries provided by fftw.org.

556

557 **4.4.2 Migration speed reduction by corridor approach**

558 It is to be expected, that any sub-cell assumption results in discretisation errors. In our case the
559 assumption of a corridor reduced the migration speed. This needs to be taken into account when
560 evaluating the result of such studies. The design of the corridors might also not have been optimal,
561 maybe a corridor wider than a single cell might result in less decrease of migration speed. However,
562 these types of analysis are outside the scope of this study. One other aspect of using the corridors is
563 that while a late successional species (in our case *F. sylvatica*) has certainly no problems to establish
564 below the early successional species, in the case of an early successional species (e.g. *B. pendula*)
565 migrating into an area occupied by a late successional species, the corridors might decrease the
566 migration speed even more. An early successional species can only establish after sufficient light
567 reaches the ground, either due to the senescence of a tree of the established species or a disturbance
568 event. The narrow corridors might have strongly limited the availability of such grid cells. However
569 since early successional species have typically a good dispersal ability, this should not influence
570 simulations of tree migration following climate change (e.g. after the last glaciation).

571 **4.4.3 Parameterisation of dispersal kernels and other plant parameters**

572 In this study the focus was on developing and testing the novel methods, i.e. we did not attempt to
573 correctly simulate the spread of *F. sylvatica* over a defined time period. The calculated spread rates
574 were well below most of the spread rates in the literature. *F. sylvatica* has been estimated to migrate
575 with ca 100 m per year based on pollen analyses by Bradshaw and Lindbladh (2005). Although such
576 estimated high migration speeds could also be the result of glacial refugia located further north than
577 assumed (Feurdean et al., 2013), our estimates of the migration speeds of 20-30 m/year still seem
578 rather low. However, in this paper we aimed to implement tree migration by using the
579 parameterisation of TreeMig in a DGVM and thereby allow large scale simulations. Our estimated
580 migration rates of 20-30 m per year are very close to the migration rates estimated for this
581 parameterisation for TreeMig by Meier et al., (2012) which estimated a value of 22 m per year. Hence,
582 though we implemented the migration module into a conceptually very different model, the resulting
583 migration rate remained relatively similar.

584 To perform model runs estimating the migration speed of any species would require a fine tuning of
585 the, age of maturity, seed production, dispersal parameters, germination rates, and seed survival
586 (which are very rough estimates in TreeMig; Lischke et al., 2006) to generate the observed migration
587 e.g. by comparing to migration rates based on pollen records. Unfortunately, though all of these
588 parameters are most likely strongly influencing the migration rates, they are not only hard to find in a

589 study performed with similar methods for all tree species, they are likely to be highly variable
590 depending on growth conditions and even provenance of the individual tree. However for a large scale
591 application at least the sensitivity of these parameters should be evaluated.

592 In our model, we assumed seed production to start at a fixed, species specific height of maturity which
593 accounts for a developmental threshold, but also growth and thus for environmental conditions
594 (similar to TreeMig, Lischke et al.2006). Other studies used age of maturity as a trigger to start seed
595 production, which has been shown to be important to determine tree migration rates (e.g. Nathan et al.,
596 2011). The aim of this study was not a full sensitivity analysis but a study showing that a similar
597 approach as Lischke et al. (2006) results in comparable migration rates. We will implement the option
598 to use age of maturity in the next version of LPJ-GM.

599 Applications of our approach to simulate migration in the future are only suitable if the migration
600 speed of any species is substantially faster than the migration speed that we reach for *F. sylvatica* (due
601 to time period for which climate projections are available). Furthermore, independent of the used
602 model, migration simulations are only suitable if the species are not typically planted, as in many
603 commercial forests.

604 **4.5 Potential for applications**

605 The test simulations were performed at a virtual landscape of 100km by 100km, but eventually the
606 method is aimed to allow large scale simulations over several millennia. Regarding memory
607 requirements, this is possible of currently available hardware: Test runs with landscapes of 4000 by
608 4000 grid cells (i.e. the size of Europe) performed without technical problems at least regarding the
609 memory requirement (given 62 GB of RAM). The considerable computational cost however requires a
610 relatively high amount of computing time, which might be reduced by efforts for speeding up (due to
611 efficient parallelisation) of the FFTM (currently the FFTM is performed on a single node while the
612 remaining nodes are idle, one could use all nodes to perform the FFTM) or by even further apart
613 corridors.

614 **5. Conclusions**

615 The presented novel approaches offer high potential to simulate the spatiotemporal dynamics of
616 species which are migrating and interacting with each other simultaneously. The approaches are not
617 restricted to LPJ-GUESS, but can in principle be applied to other DGVMs or FLMs which simulate
618 seed (or seedling) production and explicit regeneration. The presented methods need to be improved in
619 terms of computing performance to allow simulations of tree migration at continental scale and over
620 paleo time scales. Our study also shows that the estimates for seed dispersal kernels for the major tree
621 species need to be revised to allow simulations of forest development for example over the Holocene.

622 **6. Author contributions**

623 VL, DL and HL designed the study, VL performed the simulations and the statistical analysis. MM
624 and EL contributed to the study design, MM also performed large parts of the coding. EL developed
625 the formal proof in Supplementary material S.1 and the computation performance related estimates in
626 the Conclusion section. All authors contributed to the writing of the article.

627 **7. Competing interests**

628 The authors declare that they have no conflict of interest.

629 **8. Acknowledgements**

630 This study was funded by the Swiss National Science Foundation project CompMig, Nr .
631 205321_163223 .

632 **9. Code and Data availability**

633 The code generating the figures in Supplementary material 2 are part of the material. The used DGVM
634 LPJ-GUESS containing the migration module can be requested from the author.

635 The data behind all figures will be published on the DataGURU server (dataguru.lu.se;
636 doi:10.18161/migration_lehsten_2018) upon acceptance of the paper.

637 **10. References**

- 638
- 639 Bradshaw, R. H. W. and Lindbladh, M.: Regional spread and stand-scale establishment of *Fagus*
640 *sylvatica* and *Picea abies* in Scandinavia, *Ecology*, 86(7), 1679–1686, doi:10.1890/03-0785, 2005.
- 641 Bronstein, I.N., Semendjajew, K.A., Musiol, C., Mühlig, H.: *Taschenbuch der Mathematik*, Verlag
642 Harri Deutsch, Frankfurt am Main., 1995.
- 643 Bugmann, H. K. M., Brang, P., Elkin, C., Henne, P., Jakoby, O., Lévesque, M., Lischke, H., Psomas,
644 A., Rigling, A., Wermelinger, B. and Zimmermann, N. E.: Climate change impacts on tree species,
645 forest properties, and ecosystem services, in CH2014-Impacts (2014): Toward Quantitative Scenarios
646 of Climate Change Impacts in Switzerland, edited by O. (Meteoswiss) Foen., 2014.
- 647 Clarke, L., Glendinning, I. and Hempel, R.: The MPI Message Passing Interface Standard, in
648 Programming Environments for Massively Parallel Distributed Systems, edited by R. R. . Decker
649 K.M., Birkhäuser, Basel., 1994.
- 650 Cooley, J. W. and Tukey, J. W.: An Algorithm for the Machine Calculation of Complex Fourier Series

- 651 Mathematics of Computation An Algorithm for the Machine Calculation of Complex Fourier Series,
652 Source Math. Comput., 19(90), 297–301, doi:10.2307/2003354, 1965.
- 653 Dullinger, S., Willner, W., Plutzar, C., Englisch, T., Schratt-Ehrendorfer, L., Moser, D., Ertl, S., Essl,
654 F. and Niklfeld, H.: Post-glacial migration lag restricts range filling of plants in the European Alps,
655 Glob. Ecol. Biogeogr., 21(8), 829–840, doi:10.1111/j.1466-8238.2011.00732.x, 2012.
- 656 Engler, R. and Guisan, A.: MigClim: Predicting plant distribution and dispersal in a changing climate,
657 Divers. Distrib., 15(4), 590–601, doi:10.1111/j.1472-4642.2009.00566.x, 2009.
- 658 Epstein, H. E., Yu, Q. Y. Q., Kaplan, J. O. and Lischke, H.: Simulating Future Changes in Arctic and
659 Subarctic Vegetation, Comput. Sci. Eng., 9(4), 12–23, doi:10.1109/MCSE.2007.84, 2007.
- 660 Feurdean, A., Bhagwat, S. A., Willis, K. J., Birks, H. J. B., Lischke, H. and Hickler, T.: Tree
661 Migration-Rates: Narrowing the Gap between Inferred Post-Glacial Rates and Projected Rates, PLoS
662 One, 8(8), doi:10.1371/journal.pone.0071797, 2013.
- 663 Foley, J. A., Levis, S., Prentice, I. C., Pollard, D. and Thompson, S. L.: Coupling dynamic models of
664 climate and vegetation, Glob. Chang. Biol., 4(5), 561–579, doi:10.1046/j.1365-2486.1998.00168.x,
665 1998.
- 666 Gonzalez, R. C. and Woods, R. E.: Digital Image Processing, 2nd ed., Prentice Hall., 2002.
- 667 He, H. S., Gustafson, E. J. and Lischke, H.: Modeling forest landscapes in a changing climate: theory
668 and application, Landsc. Ecol., 32(7), 1299–1305, doi:10.1007/s10980-017-0529-4, 2017.
- 669 Hickler, T., Vohland, K., Feehan, J., Miller, P. A., Smith, B., Costa, L., Giesecke, T., Fronzek, S.,
670 Carter, T. R., Cramer, W., Kühn, I. and Sykes, M. T.: Projecting the future distribution of European
671 potential natural vegetation zones with a generalized, tree species-based dynamic vegetation model,
672 Glob. Ecol. Biogeogr., 21, 50–63, doi:10.1111/j.1466-8238.2010.00613.x, 2012.
- 673 Kruse, S., Gerdes, A., Kath, N. J. and Herzschuh, U.: Implementing spatially explicit seed and pollen
674 dispersal in the individual-based larch simulation model:LAVESI-WIND 1.0, Geosci. Model Dev.
675 Discuss., in review [online] Available from: <https://doi.org/10.5194/gmd-2018-%0A31>, 2018.
- 676 Lehsten, D., Dullinger, S., Huber, K., Schurgers, G., Cheddadi, R., Laborde, H., Lehsten, V., Francois,
677 L., Dury, M. and Sykes, M. T.: Modelling the Holocene migrational dynamics of *Fagus sylvatica* L.
678 and *Picea abies* (L.) H. Karst, Glob. Ecol. Biogeogr., 23(6), 658–668, doi:10.1111/geb.12145, 2014.
- 679 Lehsten, V., Sykes, M. T., Scott, A. V., Tzanopoulos, J., Kallimanis, A., Mazaris, A., Verburg, P. H.,
680 Schulp, C. J. E., Potts, S. G. and Vogiatzakis, I.: Disentangling the effects of land-use change, climate
681 and CO₂ on projected future European habitat types, Glob. Ecol. Biogeogr., 24, 653–663,

- 682 doi:10.1111/geb.12291, 2015.
- 683 Lehsten, V., Arneth, A., Spessa, A., Thonicke, K. and Moustakas, A.: The effect of fire on tree-grass
684 coexistence in savannas: A simulation study, *Int. J. Wildl. Fire*, 25(2), doi:10.1071/WF14205, 2016.
- 685 Lindeskog, M., Arneth, A., Bondeau, A., Waha, K., Seaquist, J., Olin, S. and Smith, B.: Implications
686 of accounting for land use in simulations of ecosystem carbon cycling in Africa, *Earth Syst. Dyn.*,
687 doi:10.5194/esd-4-385-2013, 2013.
- 688 Lischke, H., Löffler, T. J. and Fischlin, A.: Aggregation of individual trees and patches in forest
689 succession models: Capturing variability with height structured, random, spatial distributions, *Theor.
690 Popul. Biol.*, 54(3), 213–226, doi:10.1006/tpbi.1998.1378, 1998.
- 691 Lischke, H., Zimmermann, N. E., Bolliger, J., Riekebusch, S. and Löffler, T. J.: TreeMig: A forest-
692 landscape model for simulating spatio-temporal patterns from stand to landscape scale, *Ecol. Modell.*,
693 199(4), 409–420, doi:10.1016/j.ecolmodel.2005.11.046, 2006.
- 694 Meier, E. S., Lischke, H., Schmatz, D. R. and Zimmermann, N. E.: Climate, competition and
695 connectivity affect future migration and ranges of European trees, *Glob. Ecol. Biogeogr.*, 21(2), 164–
696 178, doi:10.1111/j.1466-8238.2011.00669.x, 2012.
- 697 Mladenoff, D. J.: LANDIS and forest landscape models, *Ecol. Modell.*, 180(1), 7–19,
698 doi:10.1016/j.ecolmodel.2004.03.016, 2004.
- 699 Nabel, J. E. M. S.: Upscaling with the dynamic two-layer classification concept (D2C): TreeMig-2L,
700 an efficient implementation of the forest-landscape model TreeMig, *Geosci. Model Dev.*, 8(11), 3563–
701 3577, doi:10.5194/gmd-8-3563-2015, 2015.
- 702 Nabel, J. E. M. S. and Lischke, H.: Upscaling of spatially explicit and linked time- and space-discrete
703 models simulating vegetation dynamics under climate change., in 27th International Conference on
704 Environmental Informatics for Environmental Protection, Sustainable Development and Risk
705 Management, EnviroInfo 2013, edited by B. Page, F. A. G. J. Göbel, and V. Wohlgemuth, pp. 842–
706 850, Hamburg., 2013.
- 707 Nathan, R., Horvitz, N., He, Y., Kuparinen, A., Schurr, F. M. and Katul, G. G.: Spread of North
708 American wind-dispersed trees in future environments, *Ecol. Lett.*, doi:10.1111/j.1461-
709 0248.2010.01573.x, 2011.
- 710 Neilson, R. P., Pitelka, L. F., Solomon, A. M., Nathan, R., Midgley, G. F., Fragoso, J. M. V, Lischke,
711 H. and Thompson, K.: Forecasting regional to global plant migration in response to climate change,
712 *Bioscience*, doi:10.1641/0006-3568(2005)055[0749:FRTGPM]2.0.CO;2, 2005.

- 713 Nobis, M. P. and Normand, S.: KISSMig - a simple model for R to account for limited migration in
714 analyses of species distributions, *Ecography* (Cop.), 37(12), 1282–1287, doi:10.1111/ecog.00930,
715 2014.
- 716 Powell, J.: Spatiotemporal models in ecology; an introduction to integro-difference equations., Utah
717 State University. [online] Available from: <http://www.math.usu.edu/powell/wauclass/labs.pdf>, 2001a.
- 718 Powell, J.: Spatiotemporal models in ecology; an introduction to integro-difference equations., Utah
719 State University., 2001b.
- 720 Pueyo, Y., Kefi, S., Alados, C. L. and Rietkerk, M.: Dispersal strategies and spatial organization of
721 vegetation in arid ecosystems, *Oikos*, doi:10.1111/j.0030-1299.2008.16735.x, 2008.
- 722 Quillet, A., Peng, C. and Garneau, M.: Toward dynamic global vegetation models for simulating
723 vegetation-climate interactions and feedbacks: recent developments, limitations, and future
724 challenges, *Environ. Rev.*, 18(NA), 333–353, doi:10.1139/A10-016, 2010.
- 725 Sato, H. and Ise, T.: Effect of plant dynamic processes on African vegetation responses to climate
726 change: Analysis using the spatially explicit individual-based dynamic global vegetation model
727 (SEIB-DGVM), *J. Geophys. Res.*, 117(G3), G03017, doi:10.1029/2012JG002056, 2012.
- 728 Sato, H., Itoh, A. and Kohyama, T.: SEIB-DGVM: A new Dynamic Global Vegetation Model using a
729 spatially explicit individual-based approach, *Ecol. Modell.*, 200(3–4), 279–307,
730 doi:10.1016/j.ecolmodel.2006.09.006, 2007.
- 731 Scherstjanoi, M., Kaplan, J. O. and Lischke, H. : Application of a computationally efficient method to
732 approximate gap model results with a probabilistic approach, *Geosci. Model Dev.*, 7, 1543–1571,
733 doi:10.5194/gmd-7-1543-2014, 2014.
- 734 Schumacher, S., Bugmann, H. and Mladenoff, D. J.: Improving the formulation of tree growth and
735 succession in a spatially explicit landscape model, *Ecol. Modell.*, 180(1), 175–194,
736 doi:10.1016/j.ecolmodel.2003.12.055, 2004.
- 737 Seidl, R., Rammer, W., Scheller, R. M. and Spies, T. A.: An individual-based process model to
738 simulate landscape-scale forest ecosystem dynamics, *Ecol. Modell.*, 231, 87–100,
739 doi:10.1016/j.ecolmodel.2012.02.015, 2012.
- 740 Shaw, M. W., Harwood, T. D., Wilkinson, M. J. and Elliott, L.: Assembling spatially explicit
741 landscape models of pollen and spore dispersal by wind for risk assessment, *Proc. R. Soc. B Biol. Sci.*,
742 doi:10.1098/rspb.2006.3491, 2006.
- 743 Shifley, S. R., He, H. S., Lischke, H., Wang, W. J., Jin, W., Gustafson, E. J., Thompson, J. R.,

- 744 Thompson, F. R., Dijk, W. D. and Yang, J.: The past and future of modeling forest dynamics: from
745 growth and yield curves to forest landscape models, *Landsc. Ecol.*, 32(7), 1307–1325,
746 doi:10.1007/s10980-017-0540-9, 2017.
- 747 Shiryaev, A. N.: *Probability*, 3rd ed., Springer Verlag, New York., 2016.
- 748 Sitch, S., Smith, B., Prentice, I. C., Arneth, A., Bondeau, A., Cramer, W., Kaplan, J. O., Levis, S.,
749 Lucht, W., Sykes, M. T., Thonicke, K. and Venevsky, S.: Evaluation of ecosystem dynamics, plant
750 geography and terrestrial carbon cycling in the LPJ dynamic global vegetation model, *Glob. Chang.
751 Biol.*, 9(2), 161–185, 2003.
- 752 Smith, B., Prentice, I. C. and Sykes, M. T.: Representation of vegetation dynamics in the modelling of
753 terrestrial ecosystems: comparing two contrasting approaches within European climate space, *Glob.
754 Ecol. Biogeogr.*, 10(6), 621–637, 2001.
- 755 Smith, B., Wärldin, D., Arneth, A., Hickler, T., Leadley, P., Siltberg, J. and Zaehle, S.: Implications of
756 incorporating N cycling and N limitations on primary production in an individual-based dynamic
757 vegetation model, *Biogeosciences*, 11(7), 2027–2054, doi:10.5194/bg-11-2027-2014, 2014.
- 758 Snell, R. S.: Simulating long-distance seed dispersal in a dynamic vegetation model, *Glob. Ecol.
759 Biogeogr.*, 23(1), 89–98, doi:10.1111/geb.12106, 2014.
- 760 Snell, R. S., Huth, A., Nabel, J. E. M. S., Bocedi, G., Travis, J. M. J., Gravel, D., Bugmann, H.,
761 Gutiérrez, A. G., Hickler, T., Higgins, S. I., Reineking, B., Scherstjanoi, M., Zurbiggen, N. and
762 Lischke, H.: Using dynamic vegetation models to simulate plant range shifts, *Ecography (Cop.)*,
763 37(12), 1184–1197, doi:10.1111/ecog.00580, 2014.
- 764 Strang, G.: Wavelets, *Am. Sci.*, 82(May-June), 250–255, 1994.
- 765 Yue, C., Ciais, P., Luyssaert, S., Li, W., McGrath, M. J., Chang, J. and Peng, S.: Representing
766 anthropogenic gross land use change, wood harvest, and forest age dynamics in a global vegetation
767 model ORCHIDEE-MICT v8.4.2, *Geosci. Model Dev.*, 11(1), 409–428, doi:10.5194/gmd-11-409-
768 2018, 2018.
- 769
- 770

771

772 **11. Contents of the supplementary material**

773

774 Derivation of the variance of the seed dispersal kernel for the SMSM S.1

775 Example evaluation of computation time difference between FFTM and the
776 traditional method S.2

777 In this appendix an example code for the FFTM is given together
778 with code demonstrating the required transformation of the seed
779 kernel for the FFTM

780

781 Example calculation of the SMSM S.3

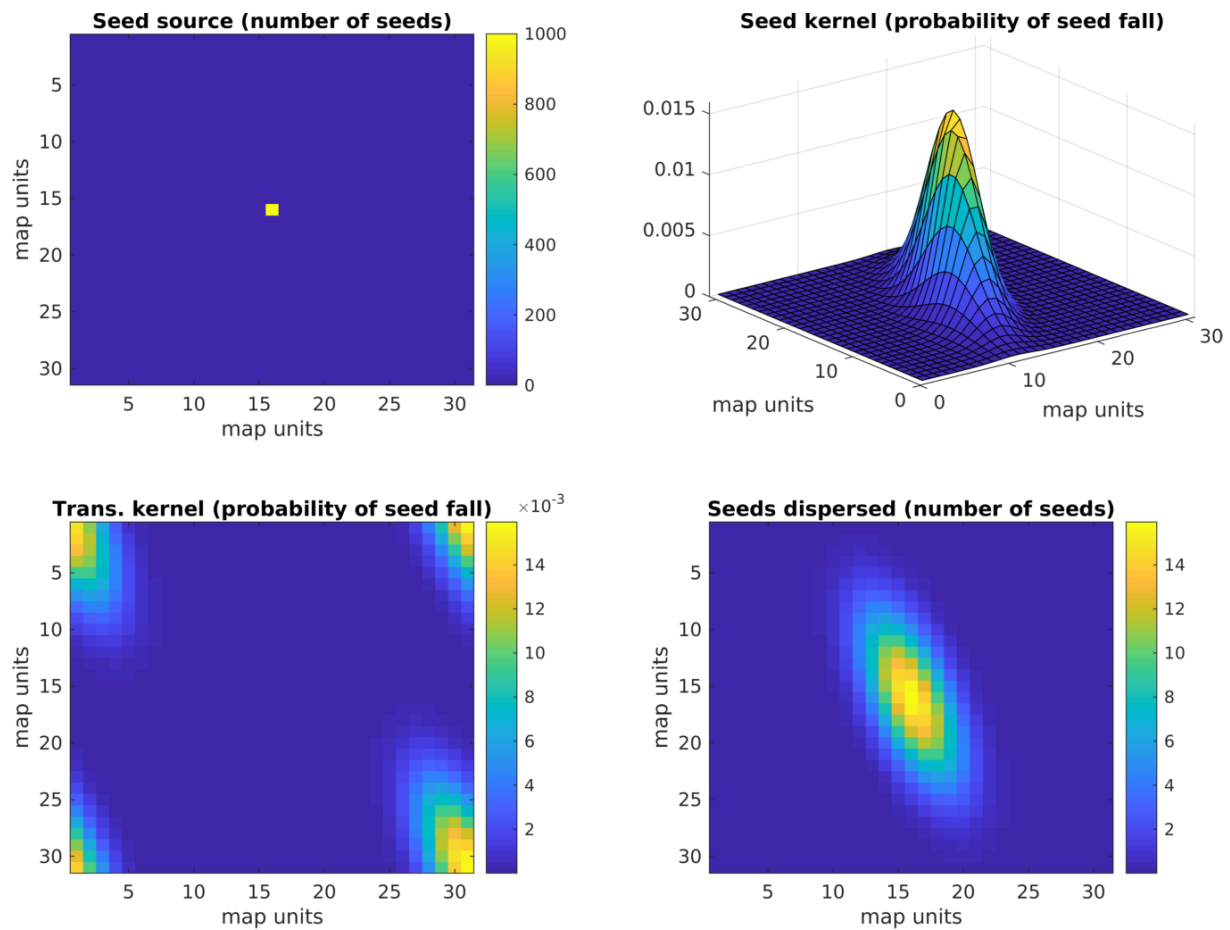
782 Species specific parameters within the simulation S.4

783

784 **12. Figures and tables**

785

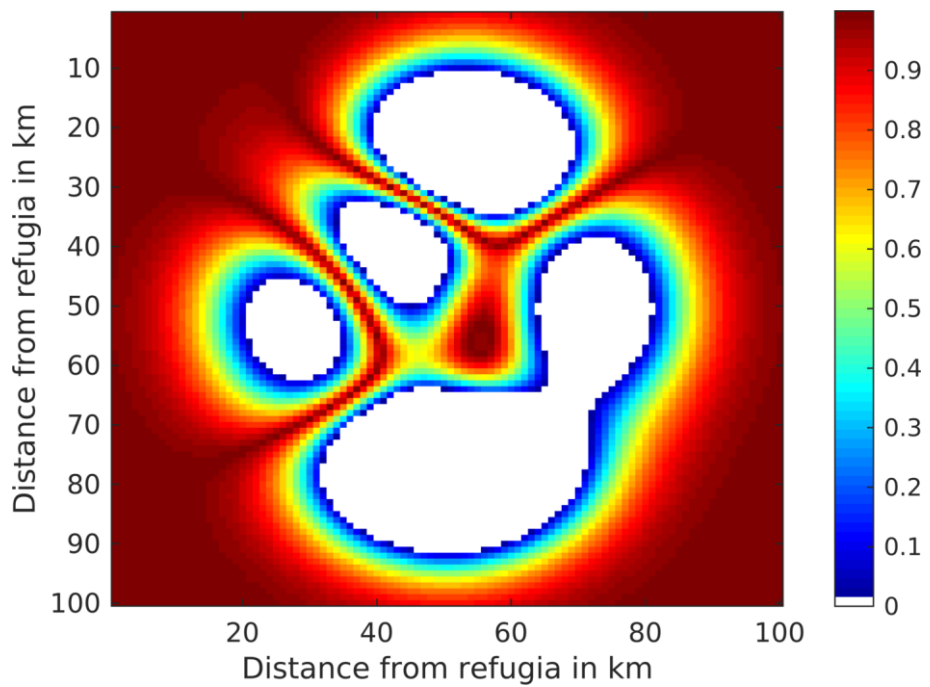
786



787

788 Fig. 1. Upper left panel: seed source. Upper right panel: example of a seed dispersal kernel (here a
789 non-symmetric kernel is assumed), lower left panel: transformed seed dispersal kernel, lower right
790 panel: seed distribution after convolution.

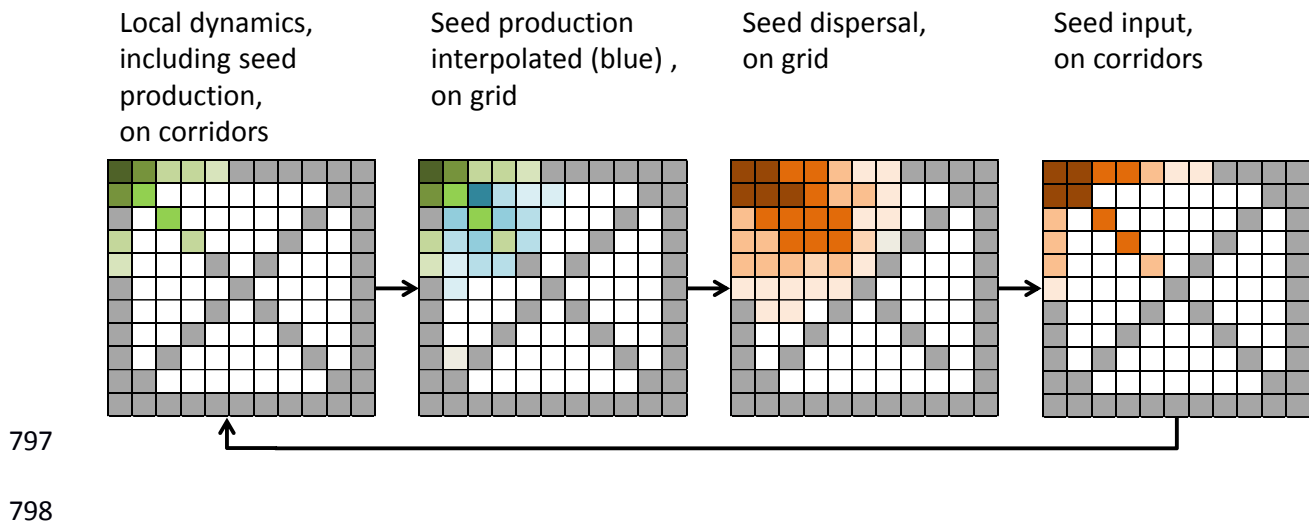
791



792

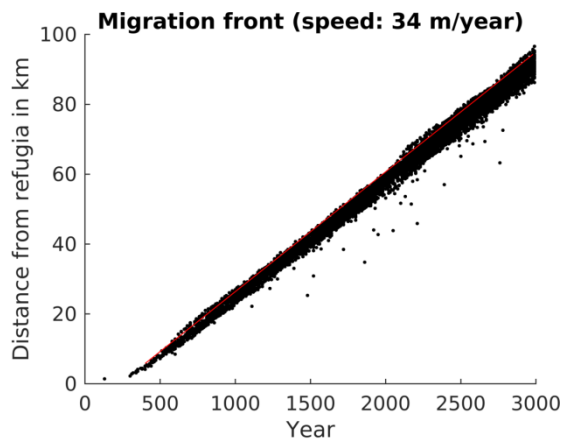
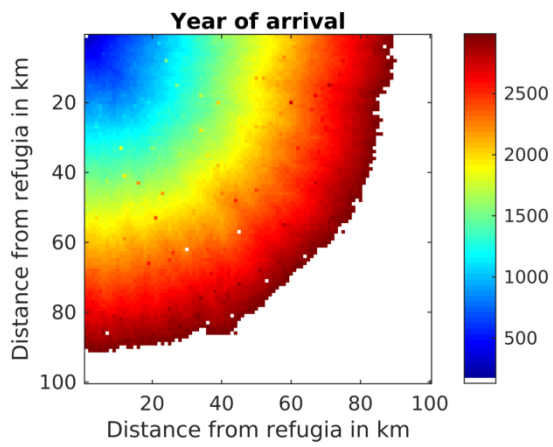
793 Fig. 2: Seed dispersal permeability for SMSM simulation tests. Each time the seed matrix is shifted,
 794 the probability of entering the new cell (which in our test is set to 5×10^{-7}) is multiplied with the seed
 795 dispersal permeability of the new potentially entered cell.

796

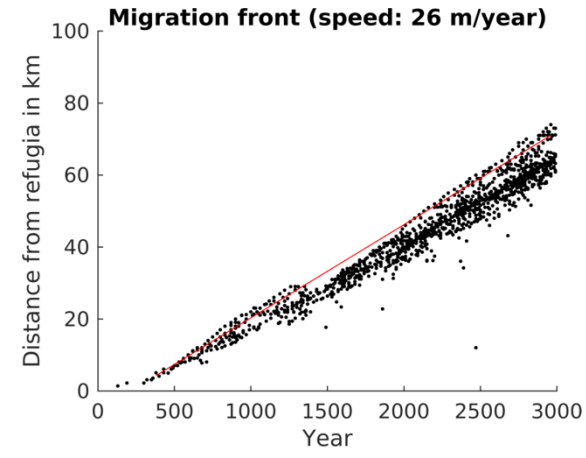
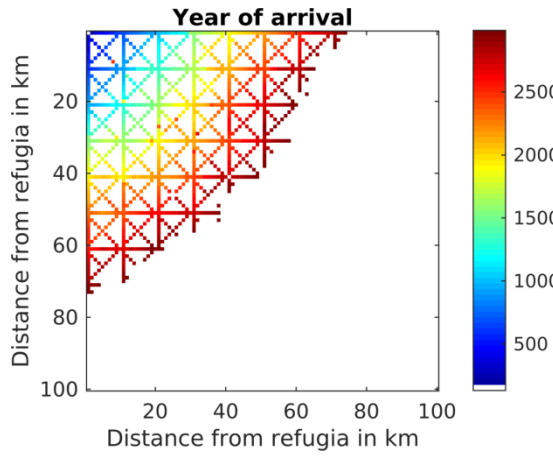


799 Fig. 3. Example of a simulated grid with transects (grey). In each time step the local vegetation
 800 dynamics including the seed production (green) is calculated on the transects. Then the seed
 801 production of each species is interpolated from the transects to all non-transect grid cells (blue) and
 802 then dispersed on the entire grid (brown). The seed input on the transect cell then enters the local
 803 dynamics in the next time step.

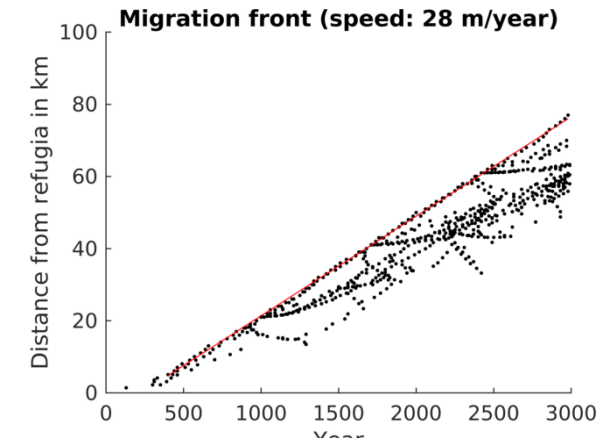
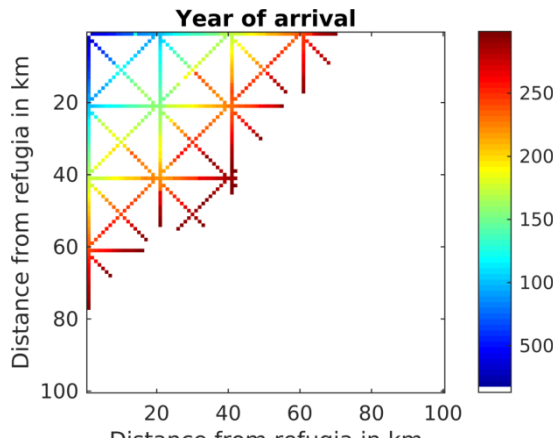
804



805



806



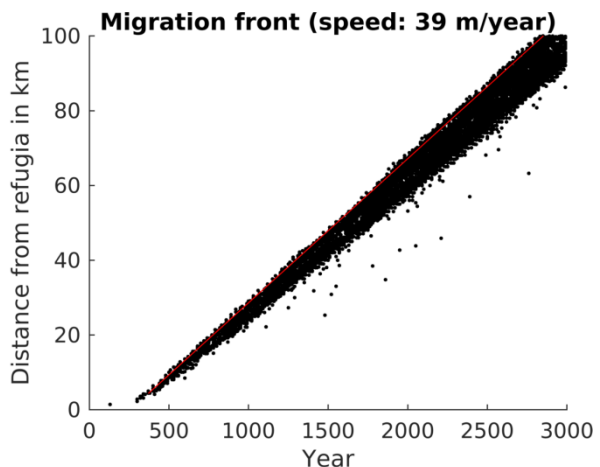
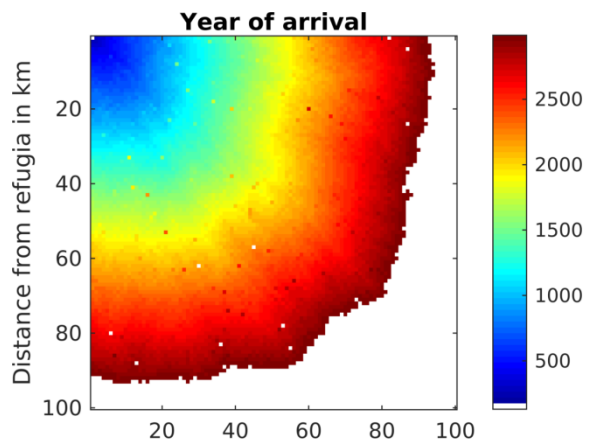
807

808 Fig. 4 Spread of *Fagus sylvatica* through an area of 100 * 100 grid cells with static climate using the

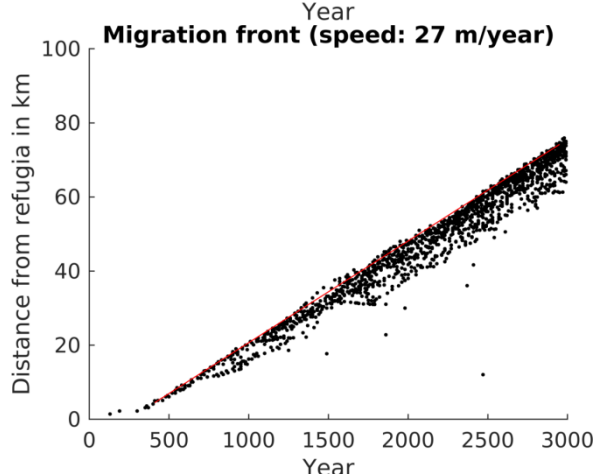
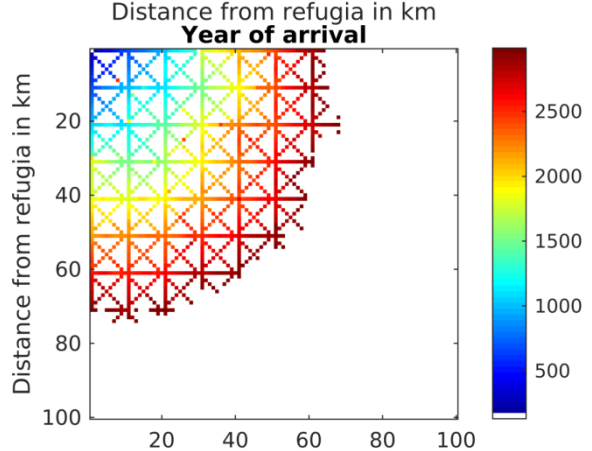
809 FFTM algorithm with no corridors or corridors every 10km, 20km or 50km. The left panels display
810 the time when *F. sylvatica* first reached an LAI of 0.5. *F. sylvatica* is allowed to establish freely only
811 in the upper left corner. The right panels show the distance of the grid cells with LAI 0.5 for *F.*
812 *sylvatica* from the starting point. The red line indicates the 95 percentile of the grid cells farthest away
813 from the starting point. The migration speed is calculated as slope of this line, taking only grid cells at
814 least 5 km away from the starting point into account to avoid some initial establishing effects.

815

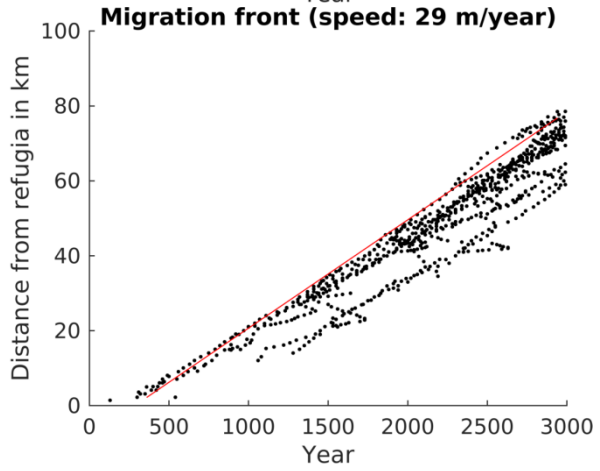
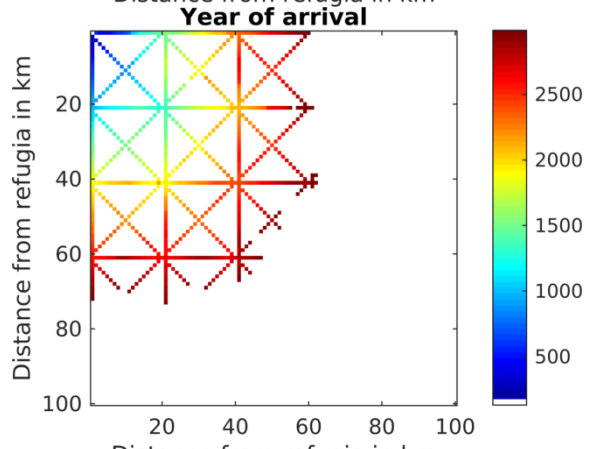
816



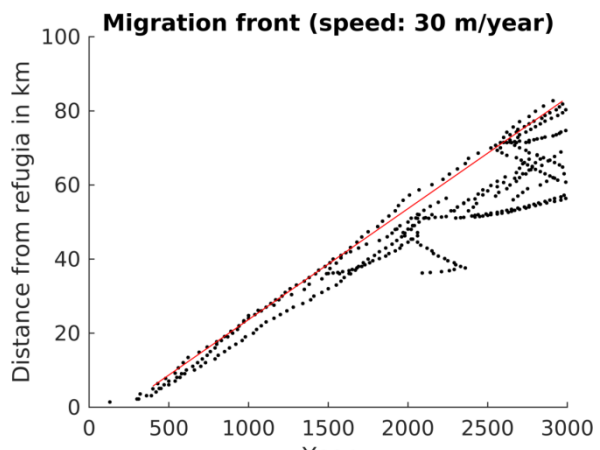
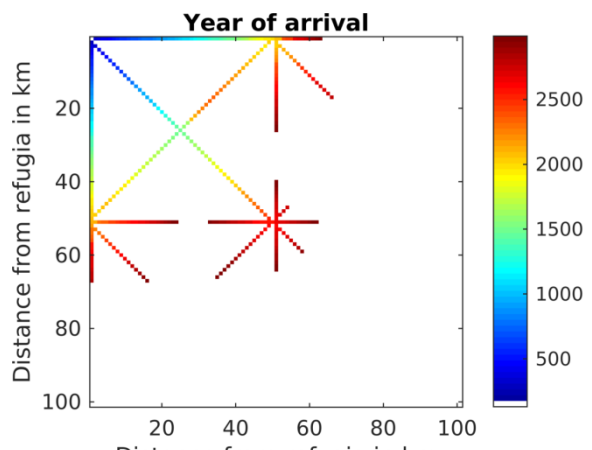
817



818

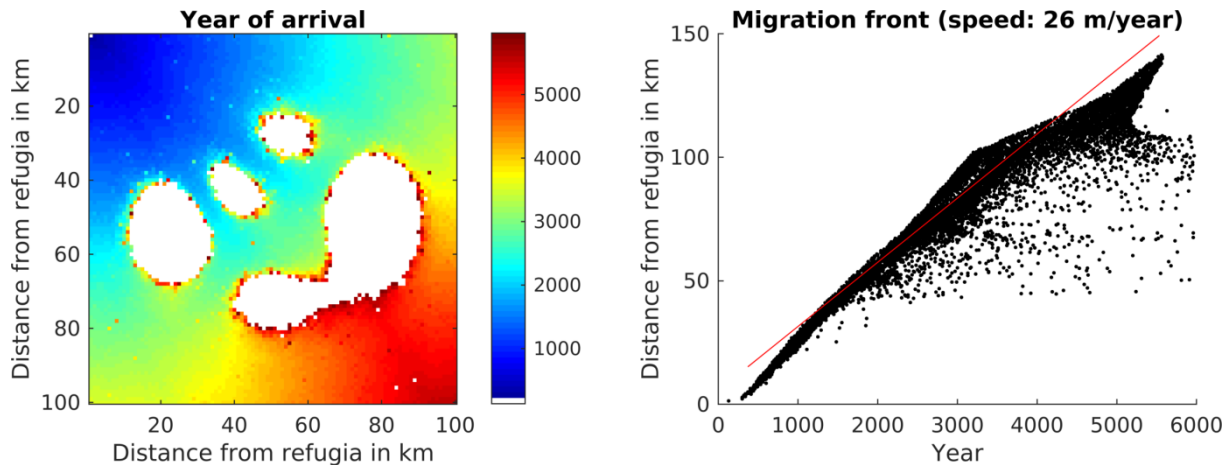


819



820 Fig. 5 Spread of *Fagus sylvatica* using the SMSM through an area of 100 * 100 grid cells with
821 identical climate, using the full area (upper row of panels) or corridors every 10th, 20th or 50th cell. For
822 more explanation see Fig. 3.

823



824
825 Fig. 6 Spread of *Fagus sylvatica* using the SMSM method through an area of 100×100 grid cells with
826 identical climate but probability of seed fall is set to 0.00005 multiplied with the spatially explicit seed
827 dispersal permeability value as shown in Fig. 2. Note that we increased the simulation time to 6000
828 years in order to have *F. sylvatica* establishing in all areas.

829

830 Table 1. Summary of migration speeds and calculation time. A corridor distance of 0 indicates no
 831 corridors but an area completely filled with grid cells. The simulated grid cells column lists the
 832 number of cells for which LPJ-GM calculates the population dynamics, in all simulations the
 833 simulation domain (for which the seed dispersal was calculated) had a size of 10000 grid cells and all
 834 simulations were performed over 3000 years. The last line lists a simulation identical to the others
 835 except that no seed dispersal was calculated to allow estimating the computation time demand for this
 836 operation.

Seed dispersal mode	Corridor distance (cells)	Simulated grid cells (corridor cells)	Migration speed, m/year	Computation time (CPU h)	Comp. time change per corridor grid cell compared to sim. without dispersal (CPU h)	Total comp. time change for whole domain compared to sim. without dispersal (CPU h)	Percentage of CPU time for dispersal	Decrease due to corridor simulation
FFTM	0	10000	34	1800	+12%	+12%	11%	
FFTM	10	3330	26	650	+22%	-59%	18%	64%
FFTM	20	1765	28	400	+41%	-75%	29%	78%
FFTM	50	977	27	220	+41%	-86%	29%	88%
SMSM	0	10000	39	2000	+25%	+19%	16%	
SMSM	10	3330	27	700	+31%	-59%	19%	65%
SMSM	20	1765	29	400	+41%	-77%	23%	81%
SMSM	50	977	30	220	+41%	-86%	32%	89%
Non	0	10000	0	1600	0%	0%	0%	

837